International Journal of Nanomedicine

Dovepress
open access to scientific and medical research

Open Access Full Text Article

ORIGINAL RESEARCH

Encapsulated *n*-Butylidenephthalide Efficiently Crosses the Blood–Brain Barrier and Suppresses Growth of Glioblastoma

This article was published in the following Dove Press journal:
International Journal of Nanomedicine

Yu-Ling Lin[1,*]
Xiao-Fan Huang[2,3,*]
Kai-Fu Chang[2,3,*]
Kuang-Wen Liao[4–6]
Nu-Man Tsai[2,7]

[1]Agricultural Biotechnology Research Center, Academia Sinica, Taipei 11529, Taiwan, Republic of China; [2]Department of Medical Laboratory and Biotechnology, Chung Shan Medical University, Taichung 40201, Taiwan, Republic of China; [3]Institute of Medicine of Chung Shun Medical University, Taichung 40201, Taiwan, Republic of China; [4]Department of Biological Science and Technology, National Chiao Tung University, Hsinchu 30010, Taiwan, Republic of China; [5]Institute of Molecular Medicine and Bioengineering, National Chiao Tung University, Hsinchu 30010, Taiwan, Republic of China; [6]Graduate Institute of Medicine, College of Medicine, Kaohsiung Medical University, Kaohsiung 80708, Taiwan, Republic of China; [7]Clinical Laboratory, Chung Shan Medical University Hospital, Taichung 40201, Taiwan, Republic of China

*These authors contributed equally to this work

Background: *n*-Butylidenephthalide (BP) has anti-tumor effects on glioblastoma. However, the limitation of BP for clinical application is its unstable structure. A polycationic liposomal polyethylenimine (PEI) and polyethylene glycol (PEG) complex (LPPC) has been developed to encapsulate BP for drug structure protection. The purpose of this study was to investigate the anti-cancer effects of the BP/LPPC complex on glioblastoma in vitro and in vivo.

Methods: DBTRG-05MG tumor bearing xenograft mice were treated with BP and BP/LPPC and then their tumor sizes, survival, drug biodistribution were measured. RG2 tumor bearing F344 rats also treated with BP and BP/LPPC and then their tumor sizes by magnetic resonance imaging for evaluation blood–brain barrier (BBB) across and drug therapeutic effects. After treated with BP/LPPC in vitro, cell uptake, cell cycle and apoptotic regulators were analyzed for evaluation the therapeutic mechanism.

Results: In athymic mice, BP/LPPC could efficiently suppress tumor growth and prolong survival. In F334 rats, BP/LPPC crossed the BBB and led to tumor shrinkage. BP/LPPC promoted cell cycle arrest at the G_0/G_1 phase and triggered the extrinsic and intrinsic cell apoptosis pathways resulting cell death. BP/LPPC also efficiently suppressed VEGF, VEGFR1, VEGFR2, MMP2 and MMP9 expression.

Conclusion: BP/LPPC was rapidly and efficiently transported to the tumor area across the BBB and induced cell apoptosis, anti-angiogenetic and anti-metastatic effects in vitro and in vivo.

Keywords: glioblastoma, *n*-butylidenephthalide, blood–brain barrier, drug delivery

Background

According to the 2016 World Health Organization Classification of Tumors of the Central Nervous System, glioblastoma has been classified as a grade IV diffuse astrocytic and oligodendroglial tumors. About 90% of isocitrate dehydrogenase (IDH) wild-type glioblastoma cases are primary or neonatal glioblastoma, and are predominantly older than 55 years old.[1] Typically primary glioblastomas are fast-growing with telomerase reverse transcriptase (TRET) promoter mutations,[2] epidermal growth factor receptor (EGFR) amplification and mutations,[3] and the phosphatase and tensin homologue on chromosome 10 (PTEN) deletion.[4] Secondary glioblastomas occur in younger patients with a history of prior lower grade diffuse glioma and are characterized by IDH-mutant,[1] Mutations of p53 and the α thalassemia/mental retardation syndrome X-linked (ATRX) were found to be common in secondary glioblastomas. Additionally, glioblastoma patients are often have platelet-derived growth factor

Correspondence: Nu-Man Tsai
Department of Medical Laboratory and Biotechnology, Chung Shan Medical University, No. 110, Sec. 1, Jianguo N. Road, Taichung 40201, Taiwan
Tel +886-4-24730022 ext. 12411
Fax +886-4-23248171
Email numan@csmu.edu.tw

submit your manuscript | www.dovepress.com
DovePress
http://doi.org/10.2147/IJN.S235815

receptor (PDGFR) overexpression, and retinoblastoma (Rb) pathway abnormality.[4,5] EGFR and PDGFR signaling activates Ras-mitogen-activated protein kinase (MAPK) and phosphatidylinositol 3-kinase (PI3K)-AKT-mammalian target of rapamycin (mTOR) pathways causing glioblastoma cell proliferation and inhibition of apoptosis.[5] In forty to fifty percent of glioblastoma patients with phosphatase and tensin homolog (PTEN) mutation, PI3K-AKT-mTOR is activated which promotes cancer progression.[5] The current standard of care for patients with glioblastoma is maximum surgical resection followed by concurrent TMZ (75 mg per square meter of body-surface area per day for 6 weeks) and radiotherapy (60 Gy in 30 fractions) and then 6 cycles of adjuvant TMZ (150 to 200 mg per square meter for 5 days during each 28-day cycle).[6] Standard treatment of glioblastoma patients in the clinic improves their median survival to 14.6 months and the 2-year survival rate is 26.5%.[6] However, almost all patients undergo tumor progression and a median survival of less than 15 months. Additionally, no standard of care is established in recurrent or progressive glioblastoma.[7] These reasons indicate that the optimal chemotherapy regimen and treatment strategy for glioblastoma remains to be developed.

Chinese medicinal herbs such as *Angelica sinensis, Ligusticum chuanxiong* and *Cnidium officinale* have anti-tumor, anti-antiangiogenic and anti-metastasis activities contributed to by their functional compounds, especially *n*-butylidenephthalide (BP).[8,9] BP activities have been reported to arrest cell growth and initiate apoptosis of glioblastoma cells. BP up-regulates orphan nuclear receptor (Nur-77) expression and causes it to translocate from the nucleus to the cytosol, which leads to cytochrome c release and caspase-3-dependent apoptosis.[10,11] BP induced Nur-77-mediated apoptosis which is involved in the suppression of phosphatidylinositol 3-kinase (PI3K)/protein kinase B (AKT)/glycogen synthase kinase-3beta (GSK-3b) pathway.[10,12,13] BP also induces glioblastoma cell senescence via suppressing Sp1 expression leading to down-regulation of human telomerase reverse transcriptase (hTERT) and S-phase kinase-associated protein 2 (Skp2) transcriptional activities.[14,15] BP reduces Axl receptor tyrosine kinase which mediates the genes of epithelial-to-mesenchymal transition (EMT) and results in inhibition of tumor migration.[9] In particular, BP has the ability to accumulate in tumor tissue of the brain through permeating the blood–brain barrier (BBB) and providing efficient cancer therapy in vivo.[16] However, clinical application of BP is limited due to its unstable structure. BP dimerization under natural conditions through cycloaddition leads to oxidation or ring cleavage of the BP monomer and interferes with BP's anti-tumor activity.[17] BP changes its formation in oxygenic environments and loses its cytotoxicity.[18] In addition, BP has low bioavailability and poor pharmacokinetics in vivo due to the water insolubility. To improve the anti-tumor efficiency of BP, drug delivery nanoparticles have been developed for BP encapsulation to overcome its poor stability and increase its aqueous solubility/dispersibility[9,19,20].

LPPC is a liposome-based nanoparticle composed of polyethylene glycol (PEG) and polyethyleneimine (PEI) used for drug delivery.[21] LPPC eases the transportation of drugs into tumor cells, even drug-resistant cells, and provides excellent cytotoxicity.[22] LPPC can be administered through intravenous injection and/or transdermal treatment.[20,22,23] Both treatments display efficient tumor growth inhibition due to a large amount of drug accumulation.[20,22,23] The properties of LPPCs allow them to strongly capture antigens or immunomodulators on their surfaces and be used as an adjuvant to trigger Th2 immune responses and antibody class switch.[24] LPPCs also strongly captured antibodies for specific drug delivery[25] and captures proteins for intracellular protein therapy.[26] In our previous study, LPPC was shown to protect BP structure against protein adsorption in the blood to preserve the drug's stability and cytotoxicity during transportation.[20] However, BP/LPPC's anti-tumor mechanisms and transmission across the BBB have not yet been verified.

In this study, BP/LPPC not only inhibited the growth of subcutaneous tumors, but also performed favorable delivery of the drug across the BBB and efficiently inhibited the tumor growth in the brain. LPPC used as a drug carrier to encapsulate BP, resulted in higher cytotoxic activity than free BP used alone. This increased cytotoxic activity of BP/LPPC was attributable to its rapid transport across the cell membrane through micropinocytosis, caveolae–dependent endocytosis and clathrin-coated vesicles simultaneously. BP/LPPC was able to arrest the cell cycle at G0/G1 phase and regulate the checkpoint mechanism to induce cell apoptosis. BP/LPPC also displayed better anti-tumor, anti-angiogenesis and anti-metastasis effects than free BP.

Materials and Methods

LPPC Preparation and BP Encapsulation

The LPPCs and the BP encapsulation were prepared according to a previously described protocol. For BP encapsulation, 100 μL of BP (1 mM) (Lancaster Synthesis, Newgate,

Morecambe, UK) were added and mixed with 1 mg of LPPC violently for 15 sec and incubated for 15 min. After incubation, the mixture of BP and LPPC was centrifuged at 5900 × g for 5 min to remove the non-encapsulated BP. This procedure was conducted twice and BP/LPPC was obtained. The concentration of BP remaining in the supernatant was then measured using a fluorescence spectrophotometer (F-4500, Hitachi, Tokyo, Japan) with an excitation wavelength of 350 nm and an emission wavelength of 430 nm. The particle size and zeta potential of the BP/LPPC and empty LPPC particles were determined by a Zetasizer instrument (Zetasizer 3000HS, Malvern Instruments, Malvern, UK).

Animal Studies

Female athymic mice (5 weeks of age) and female F344 rats (170–190 g) were purchased from the National Laboratory Animal Center (Taipei, Taiwan). The experiments of DBTRG-05MG tumor bearing xenograft mice and RG2 tumor bearing F344 rats were respectively performed in Laboratory Animal Center of National Chiao Tung University (NCTU) and Chung Shan Medical University (CSMU) following the Guide for the Care and Use of Laboratory Animals and were approved by the Institutional Animal Care and Use Committee (IACUC) in NCTU (NCTU-IACUC-104034) and CSMU (CSMU-IACUC-990).

Effects of BP/LPPC on Tumor Growth of Glioblastoma

Forty nude mice were implanted s.c. with 5×10^6 DBTRG-05MG cells per mouse and randomly divided into four groups (10 mice in each group) after tumor establishment (~50 mm^3 tumor volume). The tumor-bearing mice were treated with PBS, vehicle, BP (100 mg BP/kg) or BP/LPPC (100 mg BP/kg) by intravenous (i.v.) injection every 3 days. For another set of experiments, the tumor-bearing mice (10 mice in each group) were treated with PBS, vehicle, BP (100 mg BP/kg) or BP/LPPC (100 mg BP/kg) by intratumoral (i.t.) injection every 3 days after tumor implantation for 3 days. Tumor size was measured with a caliper, and tumor volume was calculated as L × H × W ×0.5236. The animals were sacrificed by carbon dioxide when the tumor volume exceeded 2000 mm^3. The survival of experimental animals was observed and recorded every day. Tumor sections were obtained by H&E staining and photographed under a light microscope at a magnification of 400×. The BP accumulation in the tumor area was observed and photographed under a fluorescence microscope at a magnification of 400×.

To measure the anti-tumor effects of BP/LPPC on in situ tumors, the RG2 cells were injected i.c. into the striatum of syngenic rats. Twenty rats with tumor implantation were randomly divided into four groups (5 rats in each group) and then treated with BP, BP/LPPC (60 mg/kg/day) or vehicle by i.v. injection on days 3, 5 and 7 after tumor cell implantation (days 0). Following the previous study for in situ therapy of glioblastoma, rats were treated with 300 mg/kg/day by s.c. injection on days 4, 5, 6, 7 and 8 as a positive control.[16] Tumor volume was measured using 7-T magnetic resonance imaging (7 Tesla, Bruker BioSpec 70/30 MRI) in National Taiwan University (Taipei, Taiwan). Briefly, Rats were anesthetized with isoflurane and the tumors were localized using T2-weighted anatomic images (TR, 2742 ms; TE, 33 ms). Images were recorded using a field of view (FOV) of 25 × 25 mm^2, the matrix size of 256 × 256 pixels, and a slice thickness of 1 mm. Twenty-five slices were obtained every 14 seconds for 5.51 mins per rat.

Immunohistochemical Staining

Paraffin-embedded sections were obtained from the tumors treated with BP/LPPC by i.v., i.t. or i.c. injection and were processed for immunohistochemical staining. Briefly, the slides were treated with 3% hydrogen peroxide in 1× PBS for 10 min to block endogenous peroxidase activity after being dewaxed and rehydrated. Next, the sections were washed three times with PBS-T (1×PBS containing 0.1% Tween 20) for 5 min each time, and nonspecific antibody binding was blocked by 10% fetal bovine serum in PBS for 10 min at room temperature. The sections were incubated with a rabbit polyclonal PCNA, caspase 3, VEGF or VEGFR1 (1: 200 dilution, Santa Cruz Biotechnology, Santa Cruz, CA) antibody; a mouse monoclonal VEGFR2 or MMP2 antibody (1: 200 dilution, Santa Cruz Biotechnology); goat polyclonal MMP9 antibody (1: 200 dilution, Santa Cruz Biotechnology) at 4°C overnight, and the immune complexes were probed using a horseradish peroxidase-conjugated anti-mouse, anti-rabbit or anti-goat IgG secondary antibody (1: 1000 dilution; Santa Cruz Biotechnology) and visualized by diaminobenzidine (DAB). Finally, the sections were counterstained with hematoxylin, mounted, observed under a light microscope at a magnification of 400×, and photographed.

Cells and Cell Culture

Glioblastoma cell lines and normal cell lines were purchased from the Bioresources Collection and Research Center (BCRC, Hsinchu, Taiwan). DBTRG-05MG human glioblastoma cells were cultured in RPMI 1640 (Gibco/Thermo Fisher,

Waltham, MA) growth media. The RG2 rat glioblastoma cells, SVEC mouse endothelial cells and MDCK dog normal kidney cells were cultured in Dulbecco's modified Eagle's medium (DMEM, Gibco/Thermo Fisher) growth media. Both growth media were supplemented with 10% heat inactivated FBS (Gibco/Thermo Fisher), 1% sodium pyruvate (Gibco/Thermo Fisher), 1% HEPES buffer solution (Gibco/Thermo Fisher) and 1% PS (Gibco/Thermo Fisher). All cells were cultured in a humidified atmosphere of 5% CO_2 at 37°C and sub-cultured using an enzymatic procedure (0.1% trypsin, 2 mM EDTA solution).

Cytotoxicity of BP/LPPC

The glioblastoma cells or normal cells were seeded into 96-well tissue culture plates at a concentration of 5×10^3 cells/100 μL/well and 1×10^4 cells/100 μL/well overnight. The cells were subsequently treated with serial concentrations of the various agents, such as vehicle, BP, BP/LPPC, BCNU (bis-chloroethylnitrosourea or Carmustine) or TMZ (temozolomide). After 24 h of incubation, the cell viability of each cell line was determined by MTT colorimetric assay (Sigma-Aldrich, St. Louis, MO). Cell proliferation was plotted as a percentage of the untreated control, and the 50% inhibitory concentration (IC_{50}) of each reagent was determined from the dose-effect curve.

Cell Uptake Mechanism of BP/LPPC

DBTRG-05MG or RG2 cells were seeded in 24-well tissue-culture plates at a density of 2.5×10^5 cells/well for 18 h. The cells were pre-treated with Amiloride hydrochloride hydrate (AHH, 13.3 mg/mL, Sigma-Aldrich), Filipin III (FIII, 1 μg/mL, Sigma-Aldrich) or Chlorpromazine hydrochloride (CPZ, 10 μg/mL, Sigma-Aldrich) for 1 h and then the above inhibitors were removed. Subsequently, the cells were treated with BP/LPPC containing 50 μg/mL of BP at 37°C for 0, 15, 30, 45, 60 and 90 min. After incubation, the cells were harvested by 0.05% trypsin-EDTA (Gibco/Thermo Fisher) and broken by multiple frozen-thaws. BP in the LPPCs was extracted by phenol-chloroform and determined by a fluorescence spectrometer (Hitachi F-4500, Tokyo, Japan).

Cell Cycle Analysis

DBTRG-05MG or RG2 cells were treated with 60 μg/mL of BP or BP/LPPC for 12 h. After treatment, 10^6 cells were harvested by trypsinization followed by centrifugation. The cell pellets were washed with PBS twice and stained with 100 μL of staining buffer (400 μg/mL propidium iodide and 100 μL of 1000 μg/mL RNase A in PBS) at 4°C for 1 day in the dark. A total of 10,000 cells were analyzed for DNA content by flow cytometry (BD Biosciences, Franklin Lakes, NJ). The distribution of cells in the G0/G1, S and G2/M phases of the cell cycle were determined using FlowJo software.

TUNEL Assay for Apoptotic Cells

Cells (2×10^6) were seeded in a 10 cm culture dish and treated with 60 μg/mL of BP or BP/LPPC and incubated for 12 h. Apoptosis was detected by the TdT-mediated dUTP-biotin nick end labeling (TUNEL) method using an ApopTag Plus Fluorescein In Situ Apoptosis Detection Kit (Chemicon International, Temecula, CA). The cells were photographed under the fluorescence microscopy following the manufacturer's instructions, and the different treatments were compared.

Western Blot Analysis

DBTRG-05MG and RG2 cells were seeded in 10 cm culture dishes and treated with 40 μg/mL of BP/LPPC or 70 μg/mL of BP and incubated for different times. After incubation, cell pellets were resuspended in RIPA lysis buffer (50 mM Tris-HCl,150 mM NaCl, 1% NP-40, 0.1% SDS, 1 mM EGTA and 5 mM EDTA) with protease inhibitor and incubated on ice for 30 min. After centrifugation at 12,000 × g for 30 min at 4°C, total cell lysates were collected. The protein concentration of the cell lysates was measured with a bicinchoninic acid (BCA) protein assay kit (Pierce, Rockford, IL) following the manufacturer's instructions. Twenty micrograms of the cell lysates were separated by 12% sodium dodecyl sulfate–polyacrylamide gel electrophoresis (SDS–PAGE; Bio-Rad, Hercules, CA) and transferred to polyvinylidenedifluoride (PVDF) membranes (Amersham Lifesciences, Piscataway, NJ). The membranes were blocked with 5% skim milk for 1 h at room temperature, and then incubated with the respective antibodies. The antibodies included anti-p53, anti-pRb, anti-p21, anti-PCNA, anti-cdk2, anti-cdk4, anti-cyclin D, anti-cyclin B, anti-Fas, anti-Fas-L, anti-procaspase 3, anti-procaspase 8, anti-procaspase 9, anti-Bax, anti-VEGF, anti-MMP2, anti-MMP9, anti-actin (1/200 dilution; Santa Cruz Biotechnology); anti-phospho-p53 (Ser15; 1/200 dilution; Santa Cruz), and anti-phospho-RB (Ser795; 1/2000 dilution; 1/200 dilution; Santa Cruz). The immobilized primary antigen-antibody complex was detected with the respective horseradish peroxidase-conjugated anti-mouse, anti-rabbit or anti-goat IgG secondary antibodies (1/1000 dilution; Santa Cruz) for 1 h at 25°C, then visualized with an enhanced chemiluminescence (ECL) Plus chemiluminescence system

(Amersham, Arlington Heights, IL). The degree of protein expression was calculated using Image J.

Statistical Analysis

Data are presented as mean ± SE. Statistical significance was analyzed by Student's *t*-test. The survival analysis was performed using the Kaplan–Meier method. A P value of less than 0.05 was considered to be statistically significant.

Results

Anti-Tumor Effects of BP/LPPC on Subcutaneous Tumor in Mice

To examine the therapeutic effects of BP/LPPC on glioblastoma, nude mice were s.c. inoculated with DBTRG tumor and treated with BP/LPPC (100 mg/kg/day) by i.v. or intratumoral (i.t.) injection. The results showed that both BP/LPPC treatment methods significantly inhibited the tumor growth and prolonged survival compared to the control or BP only treated groups (Figure 1A and B). To verify the efficient anti-tumor effects of BP/LPPC, the accumulation of BP was determined by pathology. The results showed amounts of BP in the tumor area of the i.v. and i.t. BP/LPPC-treated group were higher than those in BP-only treated groups (Figure 1C). The biodistribution of BP also showed LPPC delivers most of the BP to the tumor area. Unencapsulated BP also accumulates in the tumor, but they still partially accumulate in the liver (Figure 1D). Additionally, BP/LPPC dramatically decreased the PCNA (a cell proliferation marker) protein expression which indicated that BP/LPPC provided anti-proliferative activity in vivo (Figure 1E). In addition, BP/LPPC treatment increased the cleavage of caspase 3 protein to induce apoptosis of tumor cells in vivo (Figure 1E). IHC results also showed that BP/LPPC treatment significantly inhibited VEGF, VEGFR1, VEGFR2, MMP2 and MMP9 expression in the tumor area (Figure 1F). These results indicate that BP/LPPC provided

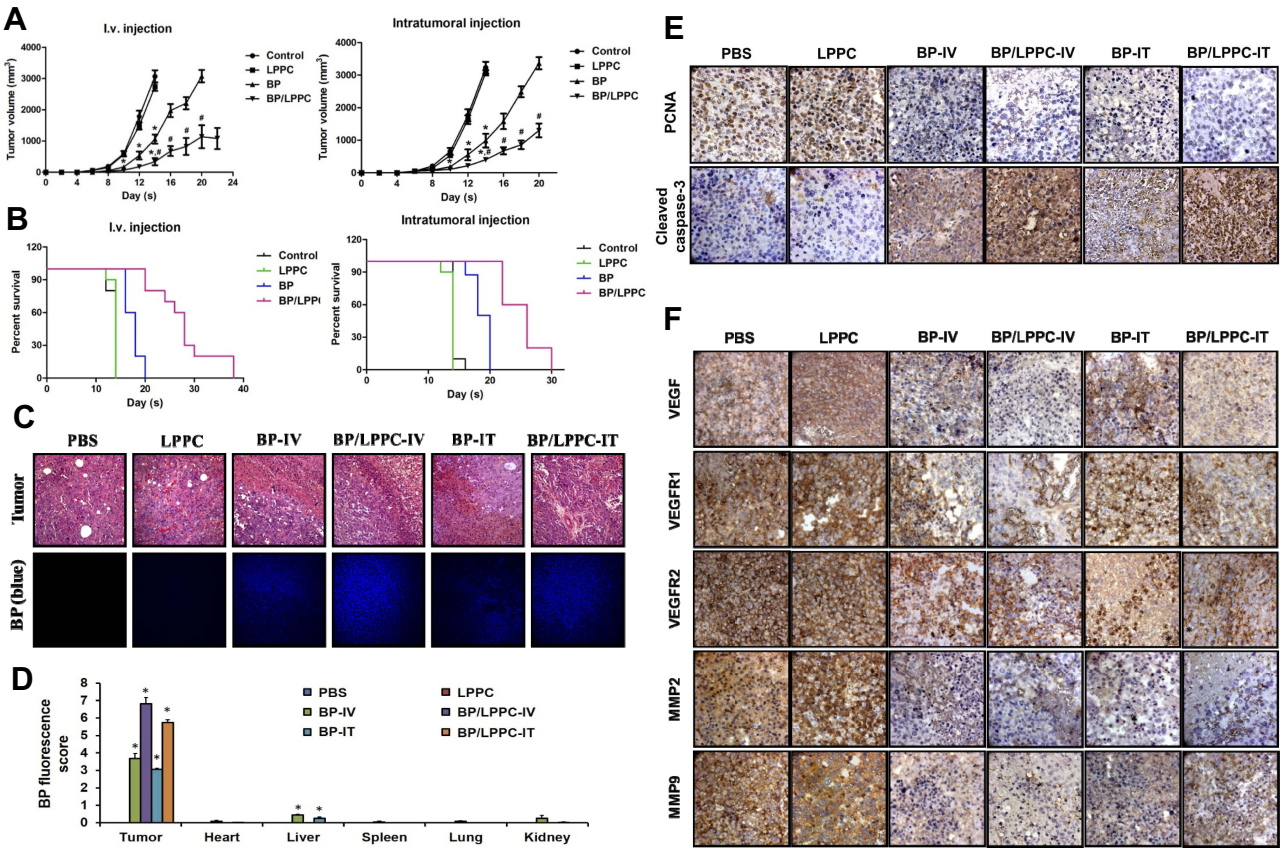

Figure 1 Anti-tumor effects of BP/LPPC in DBTRG tumor-bearing mice.

Notes: (**A**) Nude mice bearing DBTRG-05MG tumors were treated by i.v. or i.t. injection with vehicle, BP (100 mg/kg) or BP/LPPC (100 mg/kg) every 3 days. Tumor volumes were measured every 2 days (n=8). *: $P < 0.05$ compared with control group; #: $P < 0.05$ compared with BP group. (**B**) The survival of treated mice was recorded every day. (**C**) Accumulation of BP in tumors in treated mice. (**D**) Biodistribution of BP. The images were analyzed by a microscopy at 400×. Blue fluorescence indicated BP accumulation. *: $P < 0.05$ compared with PBS group. (**E**) The expression of PCNA and cleaved caspase-3 in the tumor area were observed by immunohistochemistry staining. (**F**) The expressions of VEGF, VEGFR1, VEGFR2, MMP2 and MMP9 in the tumor area were also observed by immunohistochemistry staining.

superior anti-proliferation, anti-angiogenesis and anti-metastasis effects in vivo.

Anti-Tumor Effects of BP/LPPC on Glioblastoma in situ in Rats

To investigate the anti-tumor effects of BP/LPPC on in situ glioblastoma, F344 rats were implanted i.c. (striatum) with the RG2 cells and treated with BP or BP/LPPC (60 mg/kg/day) by i.v. injection. MRI data revealed that the in-situ tumor volumes in the BP/LPPC-treated group were smaller than those in the control group and in 60% mice tumors had completely disappeared (Figure 2A). BP/LPPC significantly inhibited the tumor volume (Figure 2B) and prolonged survival (Figure 2C). Although BP treatment by i.v. or s.c. injection was able to decrease the tumor volume, BP/LPPC displayed more anti-tumor effects than BP treatment alone (Figure 2A and B). To verify the efficient anti-tumor effects of BP/LPPC, the accumulation of BP was determined by pathology. As shown in Figure 2D, a large amount of BP accumulated in tumors in BP/LPPC-treated mice. The immunohistochemistry results after BP/LPPC treatment showed a significant decrease in PCNA protein expression and an increase in cleaved caspase 3 protein expression relative to the control or BP-treated group in vivo (Figure 2E). BP/LPPC also decreased VEGF, VEGFR1 and VEGFR2 expression; these results were similar to those shown in the subcutaneous DGTRG tumor model. Therefore,

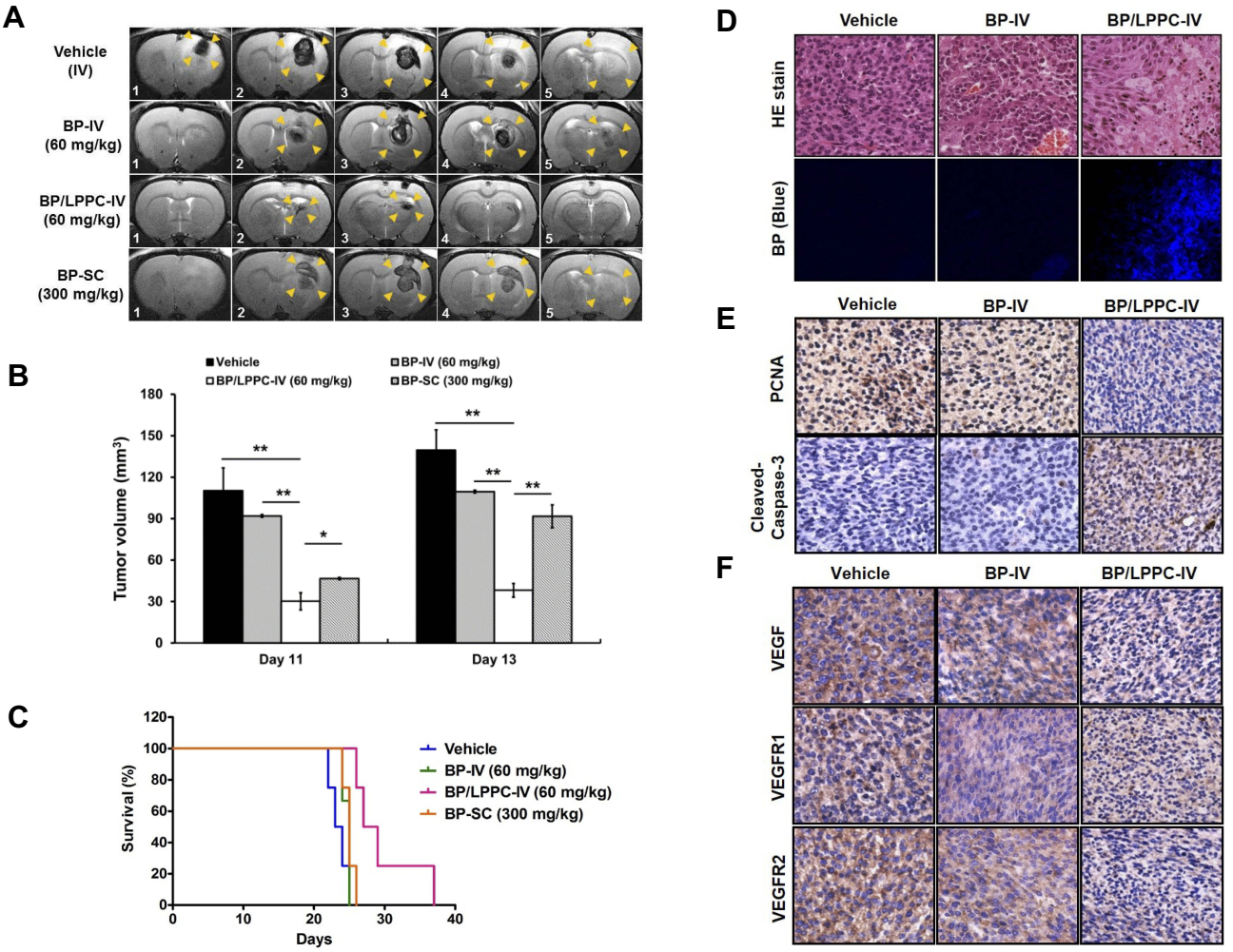

Figure 2 Anti-tumor effects of BP/LPPC in a syngenic rat glioblastoma in situ model.

Notes: RG2 cells (5×10^4) were implanted i.c. (striatum) in F344 rats. (**A**) Tumor volume shown by MRI imaging of serial sections (1.5 μm thick): Vehicle-IV 1–5 were from the control rats; BP-IV 1–5 were from BP-treated rats by i.v. injection; BP/LPPC-IV 1–5 were from BP-treated rats by i.v. injection; BP-SC1–5 were from 300 mg/kg BP-treated rats by s.c. injection. Tumor mass in each mouse is shown by the yellow arrow. (**B**) Tumor volume was calculated using echo-planar imaging capability. Each column represents mean ± SEM (n=5 in each group, $^*P < 0.05$, $^{**}P < 0.01$). (**C**) The survival of treated mice was recorded daily. (**D**) Accumulation of BP in tumors in treated rats. The images were analyzed by microscopy at 400×. Blue fluorescence indicated the BP accumulation. (**E**) PCNA and cleaved caspase-3 and (**F**) VEGF, VEGFR1 and VEGFR2 expression in BP/LPPC treated rats. Immunohistochemical staining was performed in rat brain tumor tissues on day 13 after treatment at 400×.

LPPC efficiently helped BP transit cross the blood-brain-barrier and provided high cytotoxicity in glioblastoma in situ.

In vitro Cytotoxicity

To determine the cytotoxicity of BP/LPPC, different glioblastoma cell lines were analyzed for cell viability after BP or BP/LPPC treatment. The results in Table 1 showed that the IC_{50} levels of non-encapsulated BP in DBTRG-05MG and RG2 cells were 40.6 μg/mL and 45.6 μg/mL. Compared to the non-encapsulated BP, the cells treated with BP/LPPC resulted in a lower IC_{50}; 8.6 μg/mL (DBTRG-05MG cells) and 3.8 μg/mL (RG2 cells). In addition, the IC_{50} levels of BP/LPPC in SVEC4-10 and MDCK cells were 35 μg/mL and 38.7 μg/mL (Table 1), respectively, which was 4.6 to 10-fold higher than for glioblastoma cells. For the clinical chemotherapeutic drugs BCNU and TMZ, IC_{50} levels were 65.8 μg/mL and 127.1 μg/mL in DBTRG-05MG cells; 52.2 μg/mL and 118.8 μg/mL in RG2 cells, respectively. Thus, BP/LPPC conferred higher cytotoxic activity than BP alone, BCNU and TMZ.

Cell Uptake Mechanism of BP/LPPC

To verify the cell uptake mechanism of BP/LPPC, three inhibitors AHH, FIII and CPZ were pre-treated before BP/LPPC uptake. The results in Figure 3 showed both types of cell rapidly up-take BP/LPPC within 15 mins, but all the inhibitors subsequently decrease the cell uptake of BP/LPPC. These results indicate that the three endocytic pathways, micropinocytosis, caveolae–dependent endocytosis and clathrin-coated vesicles involved in the BP/LPPC uptake are distinct.

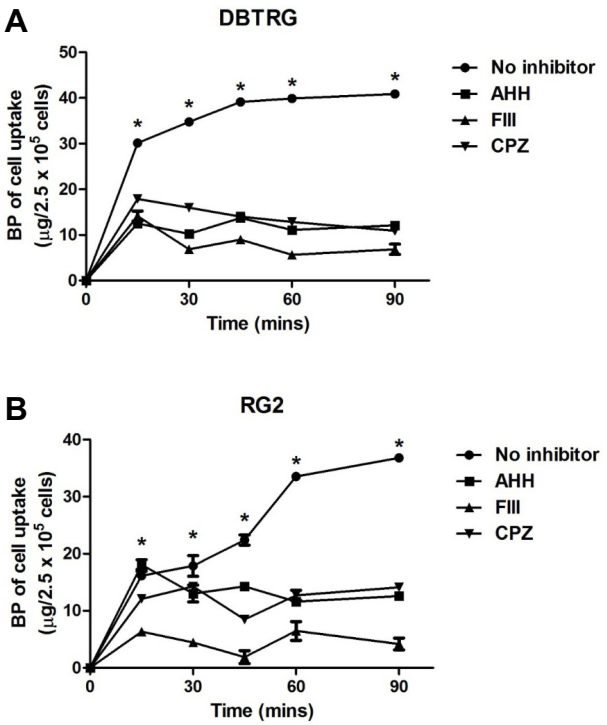

Figure 3 Uptake of BP/LPPC complex in glioblastoma cells.
Notes: (**A**) DBTRG-05MG or (**B**) RG2 cells were pre-treated with AHH, FIII or CPZ for 1 h and treated w/o BP/LPPC. Amount of BP in the cells was measured (n=3). *: $P<0.05$ compared with all inhibitor-treated groups.

Effects of BP/LPPC on Cell Cycle in Glioblastoma Cells

Cell cycle analysis of glioblastoma cells showed that treatment with BP or BP/LPPC resulted in cell cycle arrest at the G0/G1 phase (Figure 4A and B) and sub-G1 phase (Figure 1C). BP/LPPC induced a significant proportion of cells to arrest at the G0/G1 phase, which was accompanied by a concurrent decrease in the proportion of cells in S phase (Figure 4A and B). In addition, BP/LPPC caused

Table 1 Cytotoxicity of BP/LPPC (IC_{50}) in Different Brain Tumor and Normal Cells

Cell Line	Tumor Type	BP (μg/mL)	BP/LPPC (μg/mL)	BCNU (μg/mL)	TMZ (μg/mL)
Brain tumor					
DBTRG-05MG	Human glioblastoma	40.6 ± 2.3	8.6 ± 2.4[a,b,c,d]	65.8 ± 0.7	127.1 ± 4.3
RG2	Rat glioblastoma	45.6 ± 0.6	3.8 ± 1.0[a,b,c,d]	52.2 ± 0.5	118.8 ± 24
Normal cells					
SVEC	Mouse endothelial cells	74.8 ± 0.8	35.0 ± 1.9	92.8 ± 1.2	136.1 ± 2.9
MDCK	Dog normal kidney cells	136.0 ± 1.3	38.7 ± 1.8	117.7 ± 3.9	>150

Notes: All values are mean ± SD (n=3). [a]Significant difference compared with the BP treatment group. [b]Significant difference compared with the BCNU treatment group. [c]Significant difference compared with the TMZ treatment group. [d]Significant difference compared with normal cells ($P < 0.05$).
Abbreviations: BP, n-butylidenephthalide; LPPC, Lipo-PEG-PEI complex; BCNU, bis-chloroethylnitrosourea or Carmustine; TMZ, temozolomide. IC_{50}, half maximal inhibitory concentration.

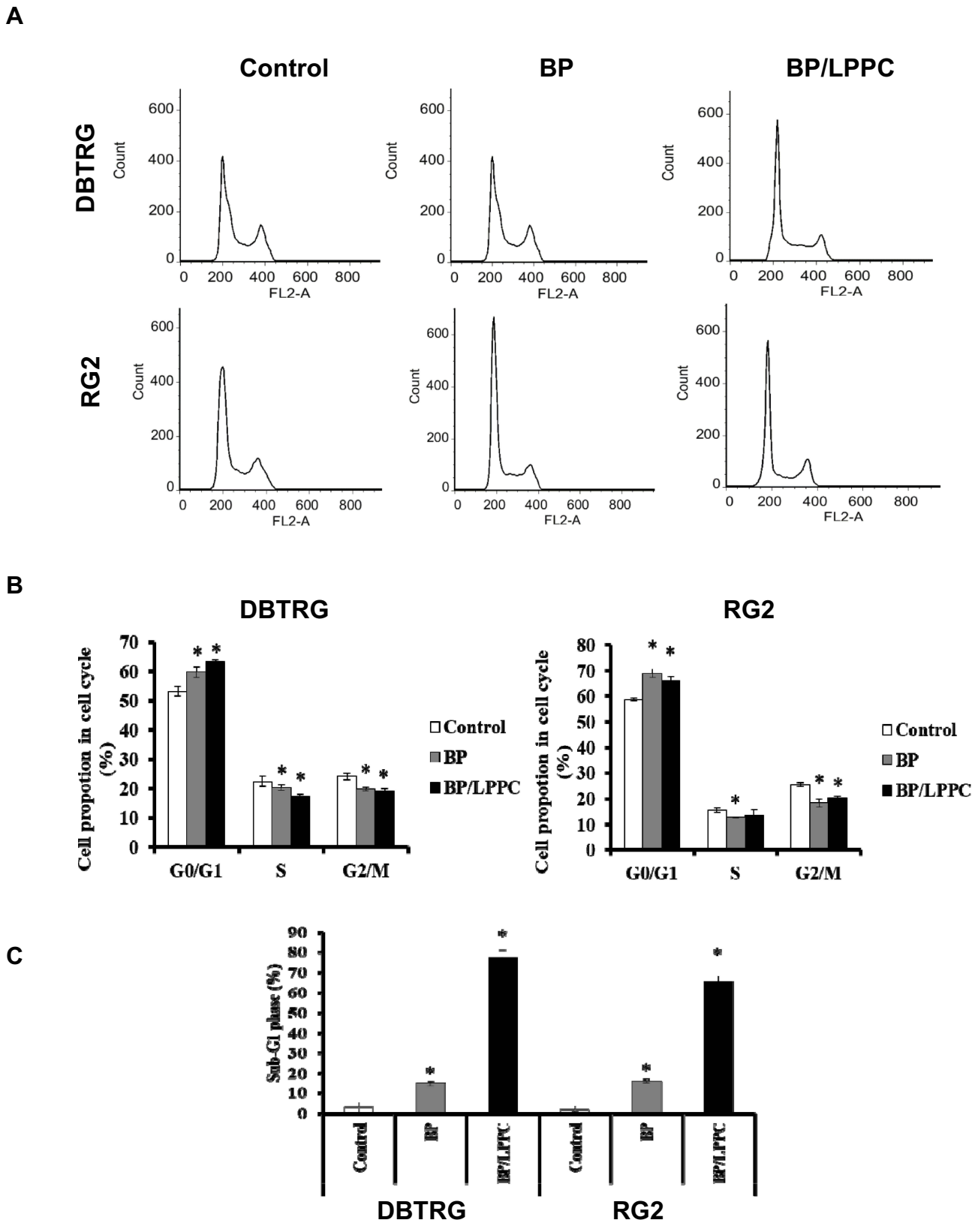

Figure 4 BP/LPPC-induced cell-cycle arrest and apoptosis in glioblastoma cells.

Notes: (**A**) DBTRG-05MG and RG2 cells were arrested in the G_0/G_1 phase with BP or BP/LPPC treatment. The proportions of cells at (**B**) G0/G1, S and G2/M phases and (**C**) after treatment. Flow cytometric analysis of DNA content in the cells treated with BP for 12 h (gray bars), cells treated with BP/LPPC for 12 h (black bars) and control cells (open bars) revealed the proportions of cells at different stages. Each column represents the mean ± SD (*$P < 0.05$).

a higher increase in the number of cells in the sub-G1 phase in both cells than BP treatment (Figure 4C).

Apoptotic Pathways Induced by BP/LPPC in Glioblastoma Cells

To determine whether the cytotoxic effects of BP/LPPC resulted from induction of apoptosis, apoptosis was analyzed by TUNEL assay. As shown in Figure 5A, BP/LPPC markedly induced apoptosis at 12 h in both types of cells. To further investigate the apoptotic pathways induced by BP/LPPC treatment, the expression of the phosphorylation of p53 and Rb proteins was first evaluated by immunoblotting. As shown in Figure 5B, total p53 protein and p-p53 increased in DBTRG-05MG cells. The p53 gene in RG2 cells was undetectable because this gene impaired and exhibited homologous deletion. The levels of phosphorylated Rb proteins were decreased after BP/LPPC treatment in both DBTRG-05MG and RG2 cells. BP/LPPC enhanced the expression of p21 but decreased the expression of CDK2, CDK4 cyclin B, and cyclin D (Figure 5B). These results indicated that BP/LPPC regulated the checkpoint of the cell cycle. The protein expressions of FAS, FASL, Bax, procaspase 8, 3, and 9 were also measured in BP/LPPC-treated glioblastoma cells. BP/LPPC increased the expression of FAS and Bax and decreased the expression of procaspase 8, 3, and 9 in these cells (Figure 5C). In addition, the activities of VEGF, MMP2 and MMP9 were determined. Figure 5C shows that BP/LPPC inhibited VEGF, MMP2 and MMP9 in both types of glioblastoma cells. These results show that BP/LPPC induced the apoptotic and anti-angiogenetic signaling more rapidly than BP. Almost all the proteins reacted with BP/LPPC after treatment for 1 h, but BP alone only showed a reaction after 6 h. Therefore, BP/LPPC exhibited rapid delivery, and a rapid effect on tumor cells.

Discussion

In this study it was shown that LPPC crossed the BBB and aided the efficient delivery of a therapeutic drug into brain tumors. BP/LPPC not only inhibited the subcutaneous tumor growth in athymic mice (Figure 1A) but also shrank the tumor in situ, even resulting in complete tumor

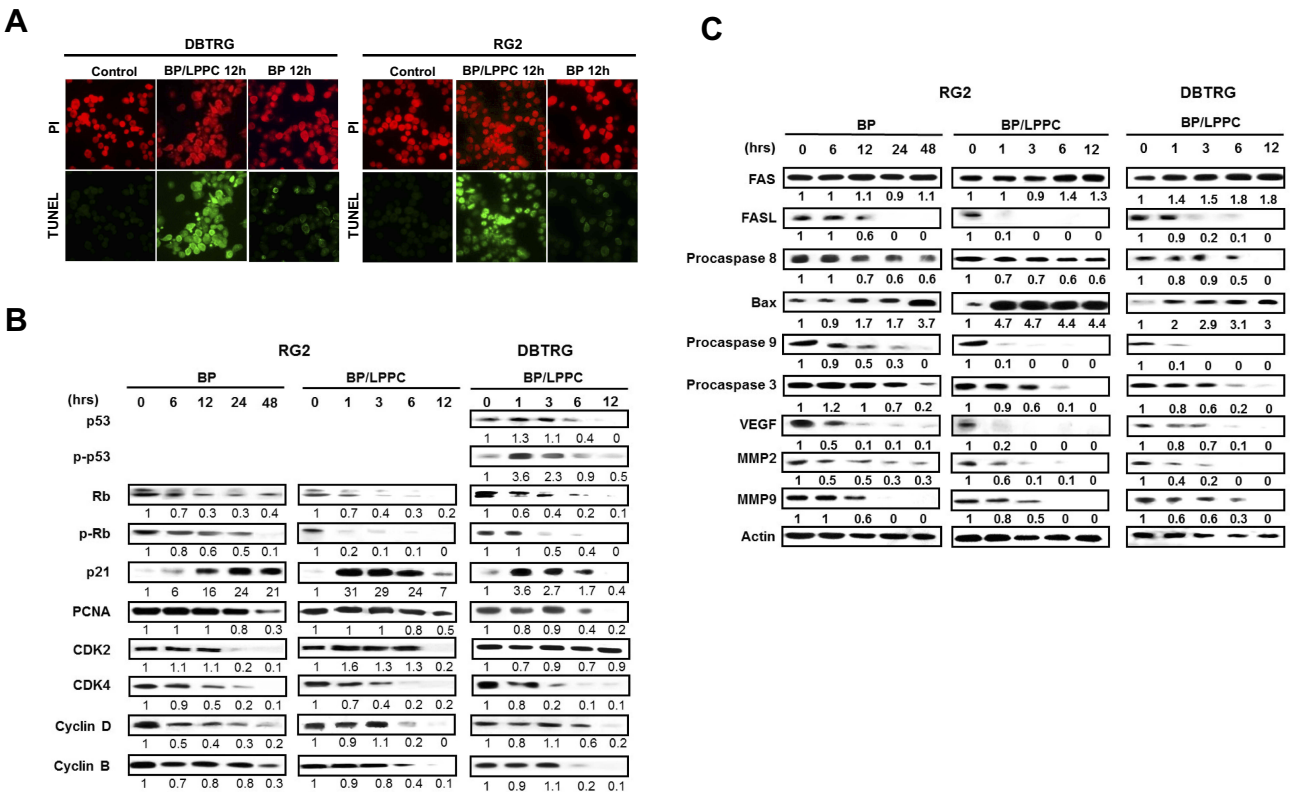

Figure 5 BP/LPPC induced apoptotic cell death and regulated the cell cycle checkpoints.

Notes: (**A**) DBTRG-05MG and RG2 cells underwent apoptotic cell death after 12 h treatment with BP or BP/LPPC. The apoptotic cells were determined by TUNEL assay for DNA fragmentation (green) and PI counterstaining for genomic DNA (red). (**B**) The expression and activation of apoptosis-associated molecules in glioblastoma cells treated with BP/LPPC. Whole cell lysates (20 μg/lane) were analyzed with Western blotting using specific antibodies to: p53, phospho-p53, Rb, phospho-Rb, p21, PCNA, cdk2, cdk4, cyclin D and cyclin B; (**C**) Fas, Fas-L, procaspase 8, Bax, procaspase 9, procaspase 3, VEGF, MMP2 and MMP9.

remission in 60% rats, thus prolonging their survival (Figure 2A and B). This excellent tumor growth inhibition resulted from effective penetration of BP/LPPC across the cell membrane that led to more BP accumulation in tumor area (Figure 1C, D and 2D) and induction of tumor cell apoptosis (Figure 1E and E). Several strategies including nanodelivery systems have been established to increase the efficiency of drug delivery across the BBB by transcellular pathways for glioma therapy.[27,28] For efficient drug delivery, penetrating peptides or transport molecules conjugated on the surface of nanoparticles enhance the uptake of nanoparticles into the brain. Although BP has been reported to pass through the BBB to suppress tumor growth because of its small molecular weight and nonpolar property, its unstable structure and low bioavailability has hitherto resulted in the limited effectiveness of BP treatment.[29] Encapsulation with LPPC overcame these limitations, and efficiently transported the drug to the tumor in situ and enhanced the cytotoxic activity of BP.

LPPC encapsulated BP was able to inhibit the glioblastoma cell proliferation and its IC_{50} was 8 to 15-fold lower than BCMU and TMZ. Compared to non-encapsulated BP, BP/LPPC significantly increased the cytotoxic activity in DBTRG and RG2 cells in vitro 4.7- and 11.9-fold, respectively (Table 1). In our previous report, it was found that LPPC encapsulation could also suppress the proliferation of drug-resistant cells and promote the cytotoxic effects of a -drug.[22] The increased cytotoxic effects of BP/LPPC may be due to its ability to rapidly cross the cell membrane through micropinocytosis, caveolae–dependent endocytosis and clathrin-coated vesicles simultaneously (Figure 3). LPPC allowed BP to efficiently accumulate in cells and induced glioblastoma cell apoptosis within 12 h (Figure 5A). Although BP/LPPC initially inhibited the proliferations of SVEC and MDCK cells, these cells recovered after 72 h treatment. Therefore, BP/LPPC efficiently suppressed the glioblastoma cell proliferation, but did not cause irreversible damage to normal cells.

BP/LPPC dramatically suppressed tumor growth by inducing cell cycle arrest at the G_0/G_1 phase and promoting apoptosis (Figure 4A–D). The mechanism of BP/LPPC was similar to that of BP alone, i.e., involvement in the cyclin/CDK/CKI cell cycle regulatory system. BP/LPPC rapidly increased phosphorylated p53 and decreased Rb expression at 1 h while the un-encapsulated BP was effective at 6 h (Figure 5B). In the clinic, mutations of p53 or Rb proteins and the components of their pathways are found in the human glioblastoma.[30,31] BP/LPPC contributed to a rapid increase in the p53 protein level that caused down-regulation of cell division. BP/LPPC also regulated p21 mediated p53-dependent G1 growth arrest by binding to cyclin D1/CDK4, or the cyclin D1/CDK6 complex, preventing the phosphorylation of the retinoblastoma (Rb) protein and resulting in G1 arrest. It has been reported that p21 inhibits cell cycle progression by two independent mechanisms, inhibition of cyclin/CDK complexes, and inhibition of PCNA function resulting in both G1 and G2 arrest.[32] BP/LPPC triggered the expression of CDK inhibitors, thus decreasing the activity of the cyclin/CDK complex and preventing Rb phosphorylation.

Fas–FasL apoptosis could be induced by BP/LPPC treatment due to the increased expression of Fas after treatment (Figure 5C). Fas is the death receptor responsible for initiating the extrinsic apoptosis pathway, which triggers the cleavage of procaspase 8 (as shown in Figure 5C, procaspase 8 was decreased), thereby enabling procaspase 3 process to induce apoptosis. BP/LPPC-induced apoptosis in glioblastoma cells also involved in the p53-dependent apoptosis pathway. The p53 protein directly activates Bax to trigger cytochrome *c* release and reduce the the mitochondrial membrane potential which results in procaspase-9 and −3 cleavage (Figure 5C). Therefore, BP/LPPC could induce cell cycle arrest at the G0/G1 phase and trigger cell apoptosis through the p53 dependent and independent apoptosis pathway in glioblastoma cells.

Radix Angelica sinensis, the source of BP, is a Chinese medicinal herb that has been used extensively in the East for the treatment of cardiovascular diseases due to its angiogenetic function. *Radix A. sinensis* contains angiogenetic modulators such as polysaccharides, ferulic acid, calycosin and calycosin-7-glucoside that may function in angiogenesis and recovery of endothelial dysfunction.[33,34] In our study the functional compound BP derived from *Radix A. sinensis* exerted anti-angiogenetic activity through downregulating VEGF, VEGFR1 and VEGFR2 expression in tumor tissue (Figure 1E and F). BP is known to suppress human umbilical vein endothelial cell proliferation, migration and capillary tube formation via the activation of p38 and ERK 1/2.[35] In this study, LPPC delivered BP across the BBB to tumor area in the brain and efficiently inhibited angiogenesis. LPPC encapsulation did not change the mechanism of anti-tumor activity of BP but enhanced its effects.

In conclusion, BP/LPPC exhibited excellent anti-cancer effects on cell-cycle arrest and apoptosis. BP/LPPC also showed potent anti-angiogenesis and anti-metastasis activity in glioblastoma. LPPC transported BP across the BBB which led to the accumulation of a large amount of BP in the tumor through clathrin dependent, caveolae-mediated and macropinocytosis uptake and triggered strong anti-cancer activity. The present results should be useful for formulation of drugs for chemotherapy of malignant brain cancers.

Acknowledgments

This work was supported in part by grants from Chung Shan Medical University Hospital Foundation (PU/CSMU-102-2). The authors thank the core facility of Zeiss LSM 510 META confocal microscopy was performed in the Instrument Center of Chung Shan Medical University, which is supported by the National Science Council, the Ministry of Education, and Chung Shan Medical University.

Disclosure

The authors declare that they have no competing interests in this work.

References

1. Louis DN, Perry A, Reifenberger G, et al. The 2016 world health organization classification of tumors of the central nervous system: a summary. *Acta Neuropathol*. 2016;131(6):803–820. doi:10.1007/s00401-016-1545-1
2. Nonoguchi N, Ohta T, Oh JE, Kim YH, Kleihues P, Ohgaki H. TERT promoter mutations in primary and secondary glioblastomas. *Acta Neuropathol*. 2013;126(6):931–937. doi:10.1007/s00401-013-1163-0
3. Watanabe K, Tachibana O, Sata K, Yonekawa Y, Kleihues P, Ohgaki H. Overexpression of the EGF receptor and p53 mutations are mutually exclusive in the evolution of primary and secondary glioblastomas. *Brain Pathol*. 1996;6(3):217–223. [discussion 223-214]. doi:10.1111/j.1750-3639.1996.tb00848.x
4. Wen PY, Kesari S. Malignant gliomas in adults. *N Engl J Med*. 2008;359(5):492–507. doi:10.1056/NEJMra0708126
5. Furnari FB, Fenton T, Bachoo RM, et al. Malignant astrocytic glioma: genetics, biology, and paths to treatment. *Genes Dev*. 2007;21(21):2683–2710. doi:10.1101/gad.1596707
6. Stupp R, Mason WP, van den Bent MJ, et al. Radiotherapy plus concomitant and adjuvant temozolomide for glioblastoma. *N Engl J Med*. 2005;352(10):987–996. doi:10.1056/NEJMoa043330
7. Weller M, van den Bent M, Hopkins K, et al. EANO guideline for the diagnosis and treatment of anaplastic gliomas and glioblastoma. *Lancet Oncol*. 2014;15(9):e395–403. doi:10.1016/S1470-2045(14)70011-7
8. Lee YM, Lee YR, Kim CS, et al. Cnidium officinale extract and butylidenephthalide inhibits retinal neovascularization in vitro and in vivo. *BMC Complement Altern Med*. 2016;16:231. doi:10.1186/s12906-016-1216-8
9. Yen SY, Chen SR, Hsieh J, et al. Biodegradable interstitial release polymer loading a novel small molecule targeting Axl receptor tyrosine kinase and reducing brain tumour migration and invasion. *Oncogene*. 2016;35(17):2156–2165. doi:10.1038/onc.2015.277
10. Chen YL, Jian MH, Lin CC, et al. The induction of orphan nuclear receptor Nur77 expression by n-butylenephthalide as pharmaceuticals on hepatocellular carcinoma cell therapy. *Mol Pharmacol*. 2008;74(4):1046–1058. doi:10.1124/mol.107.044800
11. Liu PY, Sheu JJ, Lin PC, et al. Expression of Nur77 induced by an n-butylidenephthalide derivative promotes apoptosis and inhibits cell growth in oral squamous cell carcinoma. *Invest New Drugs*. 2012;30(1):79–89. doi:10.1007/s10637-010-9518-z
12. Lin PC, Chen YL, Chiu SC, et al. Orphan nuclear receptor, Nurr-77 was a possible target gene of butylidenephthalide chemotherapy on glioblastoma multiform brain tumor. *J Neurochem*. 2008;106(3):1017–1026. doi:10.1111/j.1471-4159.2008.05432.x
13. Chang LF, Lin PC, Ho LI, et al. Overexpression of the orphan receptor Nur77 and its translocation induced by PCH4 may inhibit malignant glioma cell growth and induce cell apoptosis. *J Surg Oncol*. 2011;103(5):442–450. doi:10.1002/jso.21809
14. Huang MH, Lin SZ, Lin PC, et al. Brain tumor senescence might be mediated by downregulation of S-phase kinase-associated protein 2 via butylidenephthalide leading to decreased cell viability. *Tumour Biol*. 2014;35(5):4875–4884. doi:10.1007/s13277-014-1639-0
15. Lin PC, Lin SZ, Chen YL, et al. Butylidenephthalide suppresses human telomerase reverse transcriptase (TERT) in human glioblastomas. *Ann Surg Oncol*. 2011;18(12):3514–3527. doi:10.1245/s10434-011-1644-0
16. Tsai NM, Chen YL, Lee CC, et al. The natural compound n-butylidenephthalide derived from Angelica sinensis inhibits malignant brain tumor growth in vitro and in vivo. *J Neurochem*. 2006;99(4):1251–1262. doi:10.1111/j.1471-4159.2006.04151.x
17. Deng S, Chen SN, Yao P, et al. Serotonergic activity-guided phytochemical investigation of the roots of Angelica sinensis. *J Nat Prod*. 2006;69(4):536–541. doi:10.1021/np050301s
18. Yan R, Ko NL, Li SL, Tam YK, Lin G. Pharmacokinetics and metabolism of ligustilide, a major bioactive component in Rhizoma Chuanxiong, in the rat. *Drug Metab Dispos*. 2008;36(2):400–408. doi:10.1124/dmd.107.017707
19. Harn HJ, Lin SZ, Lin PC, et al. Local interstitial delivery of z-butylidenephthalide by polymer wafers against malignant human gliomas. *Neuro-Oncology*. 2011;13(6):635–648. doi:10.1093/neuonc/nor021
20. Lin YL, Chang KF, Huang XF, et al. Liposomal n-butylidenephthalide protects the drug from oxidation and enhances its antitumor effects in glioblastoma multiforme. *Int J Nanomedicine*. 2015;10:6009–6020. doi:10.2147/IJN.S85790
21. Liu YK, Lin YL, Chen CH, et al. A unique and potent protein binding nature of liposome containing polyethylenimine and polyethylene glycol: a nondisplaceable property. *Biotechnol Bioeng*. 2011;108(6):1318–1327. doi:10.1002/bit.23048
22. Lin YL, Liu YK, Tsai NM, et al. A Lipo-PEG-PEI complex for encapsulating curcumin that enhances its antitumor effects on curcumin-sensitive and curcumin-resistance cells. *Nanomed*. 2012;8(3):318–327. doi:10.1016/j.nano.2011.06.011
23. Lin YL, Chen CH, Wu HY, et al. Inhibition of breast cancer with transdermal tamoxifen-encapsulated lipoplex. *J Nanobiotechnology*. 2016;14:11. doi:10.1186/s12951-016-0163-3
24. Chen CH, Lin YL, Liu YK, et al. Liposome-based polymer complex as a novel adjuvant: enhancement of specific antibody production and isotype switch. *Int J Nanomedicine*. 2012;7:607–621. doi:10.2147/IJN.S28097
25. Lin YL, Tsai NM, Chen CH, et al. Specific drug delivery efficiently induced human breast tumor regression using a lipoplex by non-covalent association with anti-tumor antibodies. *J Nanobiotechnology*. 2019;17(1):25. doi:10.1186/s12951-019-0457-3
26. Lin YL, Chen CH, Liu YK, et al. Lipo-PEG-PEI complex as an intracellular transporter for protein therapeutics. *Int J Nanomedicine*. 2019;14:1119–1130. doi:10.2147/IJN.S188970

27. Wang N, Sun P, Lv M, Tong G, Jin X, Zhu X. Mustard-inspired delivery shuttle for enhanced blood-brain barrier penetration and effective drug delivery in glioma therapy. *Biomater Sci*. 2017;5:1041–1050. doi:10.1039/C7BM00133A
28. Neves AR, Queiroz JF, Lima SAC, Reis S. Apo E-functionalization of solid lipid nanoparticles enhances brain drug delivery: uptake mechanism and transport pathways. *Bioconjug Chem*. 2017;28 (4):995–1004. doi:10.1021/acs.bioconjchem.6b00705
29. Tsai NM, Lin SZ, Lee CC, et al. The antitumor effects of Angelica sinensis on malignant brain tumors in vitro and in vivo. *Clin Cancer Res*. 2005;11(9):3475–3484. doi:10.1158/1078-0432.CCR-04-1827
30. Ohgaki H, Dessen P, Jourde B, et al. Genetic pathways to glioblastoma: a population-based study. *Cancer Res*. 2004;64(19):6892–6899. doi:10.1158/0008-5472.CAN-04-1337
31. Venkatesan S, Lamfers ML, Dirven CM, Leenstra S. Genetic biomarkers of drug response for small-molecule therapeutics targeting the RTK/Ras/PI3K, p53 or Rb pathway in glioblastoma. *CNS Oncol*. 2016;5(2):77–90. doi:10.2217/cns-2015-0005
32. Cayrol C, Knibiehler M, Ducommun B. p21 binding to PCNA causes G1 and G2 cell cycle arrest in p53-deficient cells. *Oncogene*. 1998;16 (3):311–320. doi:10.1038/sj.onc.1201543
33. Yang Y, Chin A, Zhang L, Lu J, Wong RW. The role of traditional Chinese medicines in osteogenesis and angiogenesis. *Phytother Res*. 2014;28(1):1–8. doi:10.1002/ptr.4959
34. Lin PL, Li ZC, Xie RF, Wang YH, Zhou X. Compatibility study of Danggui Buxue Tang on chemical ingredients, angiogenesis and endothelial function. *Sci Rep*. 2017;7:45111. doi:10.1038/srep45111
35. Yeh JC, Cindrova-Davies T, Belleri M, et al. The natural compound n-butylidenephthalide derived from the volatile oil of Radix Angelica sinensis inhibits angiogenesis in vitro and in vivo. *Angiogenesis*. 2011;14(2):187–197. doi:10.1007/s10456-011-9202-8